Identification of surface defects in textured materials using wavelet packets

Ajay Kumar, Grantham Pang
Industrial Automation Research Laboratory
Dept. of Elec. & Electronic Engineering,
The University of Hong Kong,
Pokfulam Road, Hong Kong.
Tel:(852)-2857-8492 Fax:(852)-2559-8738
Email: gpang@hkueee.hku.hk

ABSTRACT

This paper investigates a new approach for the detection of surface defects, in textured materials, using wavelet packets. Every inspection image is decomposed with a family of real orthonormal wavelet bases. The wavelet packet coefficients from a set of dominant frequency channels containing significant information are used for the characterization of textured images. A fixed number of shift invariant measures from the wavelet packet coefficients are computed. The magnitude and position of these shift invariant measures in a quadtree representation forms the feature set for a two-layer neural network classifier. The neural net classifier classifies these feature vectors into either of defect or defect-free classes. The experimental results suggest that this proposed scheme can successfully identify the defects, and can be used for automated visual inspection

I. INTRODUCTION

Quality assurance in textured materials using surface inspection is one of the most challenging problems in machine vision. The machine vision offers accuracy, consistency, repeatability and low cost solution to the problem of subjectivity, fatigue and high cost associated with the human inspection.

A multi-resolution approach for defect segmentation using Gabor filters has been described in the previous paper [1]. Sari-Sarraf *et al.* [2] have shown the usage of texture features based on pyramid-structured wavelet transform for the inspection of textile webs.

The wavelet decomposition of an image, using pyramid-structured wavelet transform, generates a set of subimages, which contains low-frequency components of the original image. This decomposition is suitable for images in which the majority of information is concentrated in low-frequency region, *i.e.* for inspection images primarily with smooth components. However, it is not suitable for textured images where the dominant frequency channels are located in the middle frequency channels [3]. Many researchers have concluded [4] that the most significant information of texture often appears in the middle frequency bands. Hence, further decomposition in the lower frequency region by conventional wavelet transform may not help much for defect detection. Therefore an appropriate way to perform wavelet transform for textured image (such as real fabrics) is to locate dominant frequency bands and then decompose them further. This leads to the concept of tree-structured wavelet transform or wavelet packets, and has been investigated in this work for the identification of textured defects. The block diagram of this approach is shown in figure 1 and is detailed in following sections.

II. WAVELET TRANSFORM

The wavelet decomposition of a signal $f(x)$ is obtained by convolution of the signal with a family of real orthonormal basis functions $y_{p,q}(x)$:

$$f(x)y_{p,q}(x) = f(x)y_{p,q}(x)dx, \qquad (1)$$

where p and q are the integers, and are referred to as dilation and translation parameters. The basis functions $y_{p,q}(x)$ are obtained through translation and dilation of a kernel function $y(x)$ known as *mother wavelet*, *i.e.* [4],

$$y_{p,q}(x) = 2^{p/2} y(2^{p}x \quad q). \qquad (2)$$

The mother wavelet $y(x)$ can be constructed from a scaling function $f(x)$. The scaling function $f(x)$ satisfies the following two-scale difference equation [5],

$$f(x) = \sqrt{2} \sum_{k} h(k) f(2x \quad k), \qquad (3)$$

where $h(k)$ is the impulse response of a discrete filter which has to meet several conditions for the set of basis wavelet functions to be orthornormal and unique. Several different sets of coefficients of $h(k)$, satisfying the required conditions, can be found in reference [5]-[6]. The mother wavelet $y(x)$ is related to scaling function via

$$y(x) = \sqrt{2} \sum_{k} g(k) f(2x \quad k). \qquad (4)$$

0-7803-7116-X/01/$10.00 (C) 2001 IEEE

The coefficients of the filter $g(k)$ are conveniently extracted from filter $h(k)$ from the following (*quadrature mirror*) relation,

$$g(k) = (\ \ 1)^k h(1 \quad k). \tag{5}$$

The discrete filters $h(k)$ and $g(k)$ are the quadrature mirror filters (QMF), and can be used to implement a wavelet transform instead of explicitly using a wavelet function

III. WAVELET PACKETS

The wavelet packets introduced by Coifman *et al*. [7] represents the generalization of the method of multi-resolution decomposition. In pyramid-structured wavelet transform, the wavelet decomposition is recursively applied to the low frequency sub bands to generate the next level hierarchy. The key difference between the traditional pyramid algorithm and the wavelet packet algorithm is that the recursive decomposition is no longer applied to the low frequency sub-bands. Instead, it is applied to any of the frequency bands based on some criterion, leading to quadtree structure decomposition.

The concept of wavelet packet bases has been generalized to obtain multiresolution decomposition of an image. A given function, say $_0$, can be used to generate a library of wavelet packet basis functions $\{\ _q\}_{q\ N}$ as follows:

$$\begin{aligned} {}_{2q}(x) &= \sqrt{2} \quad h(k) \quad {}_q(2x \quad k), \\ {}_{2q+1}(x) &= \sqrt{2} \quad g(k) \quad {}_q(2x \quad k), \end{aligned} \tag{6}$$

where the function $_0$ and $_1$ can be identified with the scaling function f and the mother wavelet y , respectively. Equation (6) uniquely defines a library of wavelet packet bases as a set of orthonormal basis functions of the form $_q(2^l x \quad k)$. Each element in the library is determined by a subset of indices *l*, *k*, and *q*, which corresponds to the scaling, dilation, and oscillation parameters, respectively. A set of 2-D wavelet packet basis functions can be obtained from the tensor product of two separable 1-D wavelet basis functions in the horizontal and vertical directions. The corresponding 2-D filters in this set can be grouped as:

$$\begin{aligned} h_{LL}(k,l) &= h(k)h(l), \\ h_{LH}(k,l) &= h(k)g(l), \\ h_{HH}(k,l) &= g(k)g(l), \\ h_{HL}(k,l) &= g(k)h(l). \end{aligned} \tag{7}$$

As shown in figure 2, application of above four filters transforms a given image into a representation having components in four sub-bands. These four sub-bands are four subimages that contain low frequency information (approximation w_a^{j+1}) and high frequency details in horizontal (w_{d1}^{j+1}), vertical (w_{d2}^{j+1}), and diagonal (w_{d3}^{j+1}) direction. Iterating this filtering process (figure 2) to each of the given sub-bands yields quadtree-structure decomposition. The subimages in the same decomposition level provide the multiple looks of the original image in different frequency bands.

IV. METHODOLOGY

The wavelet packet decomposition of every acquired image is performed. The Daubechies minimum-support least asymmetric wavelet, of filter length 4, is used in this experiment. Daubechies wavelets are compactly supported and are orthornomal, and are one of the most widely used wavelets. The coefficients of QMF's, *i.e*. g(*k*) and *h*(*k*), are show in table 1. Full wavelet packet decomposition at every scale will produce a large number of coefficients. Therefore, only the dominant frequency channels based on Shannon's entropy criterion are used. The best-basis wavelet packet tree is computed as follows [7]-[8]:

(i) Decompose a given image into four subimages by convolution and decimation with a pair of QMF's, as shown in figure 2. The given image can be viewed as parent node and subimages as the children nodes of a tree.

(ii) Compute the Shannon's entropy (e^i) of the parent and children of this tree using equation (8).

(iii) If the sum of the entropy of four children nodes is higher than the entropy of parent node, then decomposition for this parent node is aborted.

(iv) If the sum of entropy of children nodes is lower than entropy of parent node, then above decomposition is further applied to each of the children nodes.

In this work, best-basis wavelet packet decomposition of every image at three resolution levels is used. The wavelet packet coefficients from each of the sub-images are used for the feature extraction.

A. Feature Extraction

Since the wavelet coefficients are shift-variant, they are not suitable for direct use. Instead texture features must be shift-invariant [9]. Therefore four shift-invariant measures from the elements of

wavelet packet coefficients $w^i(m,n)$ in each channel are computed as follows:

$$s^i = \frac{1}{MN} \sum_{m=1}^{M} \sum_{n=1}^{N} \left(w^i(m,n) - \mu^i\right)^2,$$

$$\text{where } m^i = \frac{1}{MN} \sum_{m=1}^{M} \sum_{n=1}^{N} w^i(m,n)$$

$$e^i = \sum_{m=1}^{M} \sum_{n=1}^{N} \left((w^i(m,n))\right)^2 \log\left((w^i(m,n)\right)^2,$$

$$a^i = \frac{1}{MN} \sum_{m=1}^{M} \sum_{n=1}^{N} \frac{\left(w^i(m,n) - \mu^i\right)^4}{(s^i)^4}, \qquad (8)$$

$$\beta^i = \frac{1}{MN} \sum_{m=1}^{M} \sum_{n=1}^{N} \frac{\left(w^i(m,n) - \mu^i\right)^3}{(s^i)^3},$$

where $w^i(m,n)$ denotes the wavelet coefficient matrix, μ^i is the mean, s^i is the standard deviation, e^i is the entropy, a^i is the kurtosis, and β^i is the skewness of the wavelet coefficient matrix for each of the i^{th} channel. Five dominant values of each of these four features and their location (integer value) on the best-basis wavelet packet tree are used as features vector for every acquired image. Thus 40 features characterize every image. Further, the KL transform is used to reduce the dimension of feature vector.

B. Neural Net classifier

A two layer feed-forward neural network with 20 input nodes and one output node is used to classify feature vectors in one of the two classes. The hyperbolic tangent sigmoid activation function with gradient descent training algorithm is employed to train the neural network. The values –1 and 1 corresponding to samples with defect and without defect were used for training.

V. EXPERIMENT AND RESULTS

Several real fabric samples were gathered from textile loom and were divided into two classes; (i) with defect and (ii) without defect. Images of these fabric samples with 256 gray levels were acquired under backlighting and covered 1.28 1.28 inch^2 area of fabric. These images were digitized into 256 256 pixels. Figure 3 shows the best basis three level wavelet packet decomposition of fabric sample (figure 5.a) with defect *mispick*. The quadtree representation of this decomposition with the respective entropy values at the nodes is shown in figure 4. The full wavelet packet decomposition of this image requires 64 nodes as compared to 31 nodes used in this work. Figure 5 shows images with 8 different categories of fabric defect used in this experiment. For every image the dimension of feature vector was reduced from 40 1 to 12 1 using KL transform. Those feature values that contributed to less than 2 % of total variance in the transformed space were neglected.

In this work 42 images from each of the two classes were used for the training and 16 images were used for the testing. Each of these 42 images (16 for testing) were composed of one of the 8 different categories of fabric defect shown in figure 5. At least 5 images from each of these categories were used for training while 2 images from each category are used for testing. The scores of neural network output from testing and training images are summarized in table 2.

VI. CONCLUSIONS

In this paper a new approach for the defect identification using wavelet packets has been investigated. The experimental results in table 2 show that the 12 fabric samples with defect, out of 16 used for testing, have been successfully detected (75 %). The defect detection results for some of the fabric defects with very subtle intensity variations, *e.g.* in figure 5(a) and 5(g), were excellent (100 % detection). The results shown in this paper are promising and suggest its application for automated visual inspection.

REFERENCES

1. Ajay Kumar and Grantham Pang, "Defect detection in textured materials using Gabor filters," *Proc. 35th IAS Annual Meeting*, Rome (Italy), 8-12 Oct. 2000.
2. H. Sari-Sarraf and J. S. Goddard, "Vision systems for on-loom fabric inspection," *IEEE Trans. Ind. Appl.*, vol. 35, pp. 1252-1259, Nov-Dec. 1999.
3. T. Randen and J. H. Husøy, "Multichannel filtering for image texture segmentation," *Opt. Eng.,* vol. 33, no. 8, pp. 2617-2625, Aug. 1994
4. T. Chang and C.C. Jay Kuo, "Texture analysis and classification with tree-stuctured wavelet transform," *IEEE Trans. Image Process.*, vol. 2, no. 4, pp. 429-441, Oct. 1993.
5. I. Daubechies, "Orthonormal bases of compactly supported wavelets," *Communications on Pure and Applied Mathematics,* vol. 35, pp. 72-98, Nov. 1988.
6. S. G. Mallat, "A theory for multiresolution signal decomposition: the wavelet representation," *IEEE Trans. Patt. Anal. Machine Intell.*, vol. 11, pp. 674-693, Jul. 1989.
7. R.R. Coifman and M.V. Wickerhauser, "Entropy-based algorithms for best basis selection," *IEEE Trans. Inf. Theory,* vol. 38, no. 2, pp. 713-718, Feb. 1992.
8. M. Lee and C. Pun, "Texture classification using dominant wavelet energy features," *Proc.4th IEEE Southwest Symp. Image analysis and Interpretation,* pp. 301-304, 2000.
9. X. Tang and W. K. Stewart, "Optical and sonar image classification: wavelet packet transform vs Fourier transform," *Comput. Vis. & Image Under.*, vol. 79, pp. 25-46, 2000.

Table 1: Coefficents Daubechies wavelet transform filter used in the experiment.

h(0)	-0.01059740	g(0)	-0.23037781
h(1)	0.03288301	g(1)	0.71484657
h(2)	0.03084138	g(2)	-0.63088076
h(3)	-0.18703481	g(3)	-0.02798376
h(4)	-0.02798376	g(4)	0.18703481
h(5)	0.63088076	g(5)	0.03084138
h(6)	0.71484657	g(6)	-0.03288301
h(7)	0.23037781	g(7)	-0.01059740

Table 2: Scores of the Neural Network output from the experiment.

SNo.- Category	**Class 1** Samples with-defect	**Class 2** Samples without-defect
1.a	-1.0060	1.0060
2.a	-1.0057	1.0041
3.b	-1.0060	0.9966
4.b	-0.9759	-0.6101
5.c	-0.9750	-1.0060
6.c	-1.0060	-0.5724
7.d	-1.0060	1.0012
8.d	-0.3366	1.0060
9.e	-1.0031	-1.0060
10.e	-0.9574	1.0001
11.f	0.1385	1.0060
12.f	1.0030	0.8704
13.g	-1.0060	1.0060
14.g	-0.9480	1.0060
15.h	1.0060	1.0005
16.h	1.0055	-0.8421

Classification rate for test images (from above data) = 71.86%
Classification rate for the training images = 100%

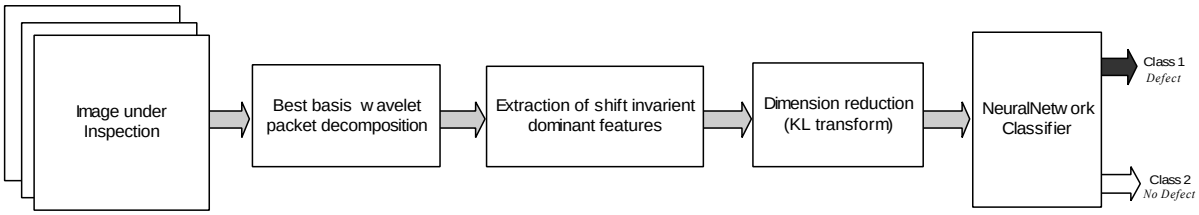

Figure 1: Block Diagram of the proposed inspection system for surface defects.

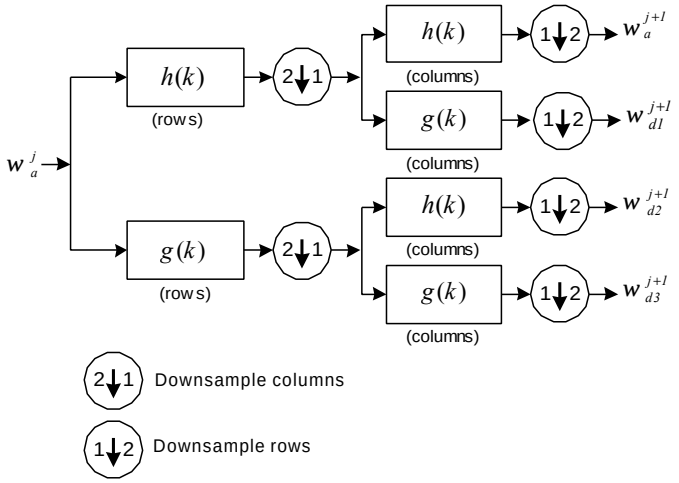

Figure 2: Multiresolution decomposition of an image using QMF.

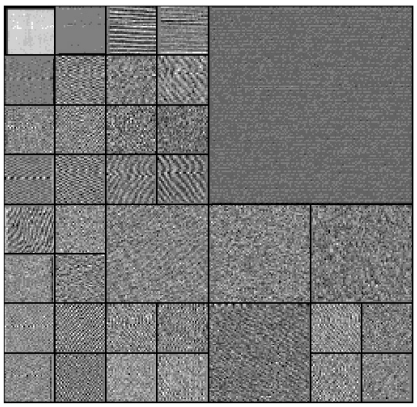

Figure 3: The best basis wavelet packet decomposition for fabric sample with defect *mispick* (figure 5.a)

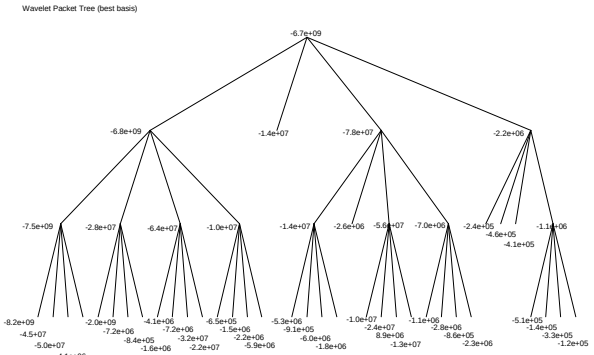

Figure 4: The Quadtree structure for best basis wavelet packet decomposition shown in figure 3.

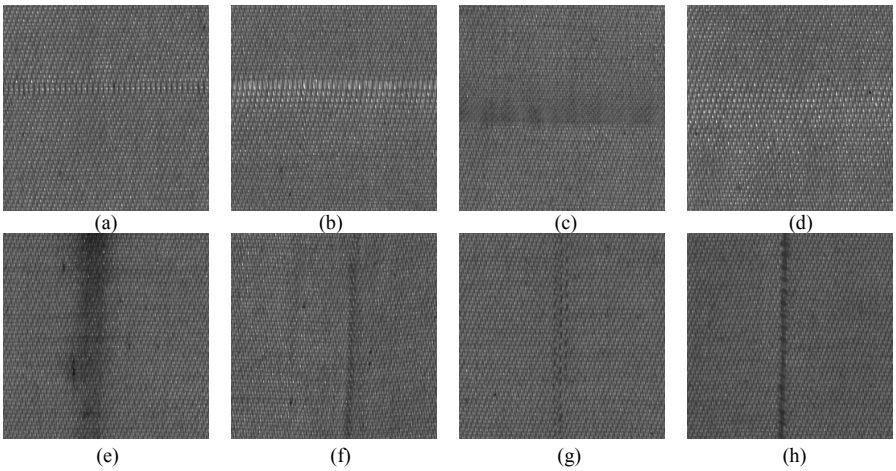

Figure 5: Fabric samples with defect of 8 categories used in the experiment